REPORTS OF PRACTICAL ONCOLOGY AND RADIOTHERAPY 22 (2017) 141–149

Available online at www.sciencedirect.com

ScienceDirect

journal homepage: http://www.elsevier.com/locate/rpor

Original research article

Imaged-guided liver stereotactic body radiotherapy using VMAT and real-time adaptive tumor gating. Concerns about technique and preliminary clinical results

Carmen Llacer-Moscardo[a,*], *Olivier Riou*[a], *David Azria*[a], *Ludovic Bedos*[a], *Norbert Ailleres*[a], *Francois Quenet*[b], *Philippe Rouanet*[b], *Marc Ychou*[c], *Pascal Fenoglietto*[a]

[a] *Department of Radiation Oncology, Montpellier Cancer Institute (ICM), Montpellier, France*
[b] *Department of Surgical Oncology, Montpellier Cancer Institute (ICM), Montpellier, France*
[c] *Department of Medical Oncology, Montpellier Cancer Institute (ICM), Montpellier, France*

ARTICLE INFO

Article history:
Received 4 February 2016
Accepted 26 June 2016
Available online 5 September 2016

Keywords:
Liver SBRT
Adaptative tumor gating
VMAT

ABSTRACT

Background: Motion management is a major challenge in abdominal SBRT. We present our study of SBRT for liver tumors using intrafraction motion review (IMR) allowing simultaneous KV information and MV delivery to synchronize the beam during gated RapidArc treatment.
Materials and methods: Between May 2012 and March 2015, 41 patients were treated by liver SBRT using gated RapidArc technique in a Varian Novalis Truebeam STx linear accelerator. PTV was created by expanding 5 mm from the ITV. Dose prescription ranged from 40 to 50 Gy in 5–10 fractions. The prescribed dose and fractionation were chosen depending on hepatic function and dosimetric results. Thirty-four patients with a minimal follow-up of six months were analyzed for local control and toxicity. Accuracy for tumor repositioning was evaluated for the first ten patients.
Results: With a median follow-up of 13 months, the treatment was well tolerated and no patient presented RILD, perforation or gastrointestinal bleeding. Acute toxicity was found in 3 patients with G1 abdominal pain, 2 with G1 nausea, 10 with G1 asthenia and 1 with G2 asthenia. 6 patients presented asymptomatic transitory perturbation of liver enzymes.

In-field local control was 90.3% with 7 complete responses, 14 partial responses and 7 stabilisations. 3 patients evolved “in field”. 12 patients had an intrahepatic progression “out of field”.

Mean intrafraction deviation of fiducials in the craneo-caudal direction was 0.91 mm (0–6 mm).
Conclusion: The clinical tolerance and oncological outcomes were favorable when using image-guided liver SBRT with real-time adaptive tumor gating.

* *Corresponding author at*: Department of radiation Oncology, Montpellier Cancer Institute (ICM), 208, Avenue des Apothicaires, Parc Euromédecine, 34298 Montpellier Cedex 5, France. Fax: +33 467613135.
E-mail address: carmen.llacer@icm.unicancer.fr (C. Llacer-Moscardo).
http://dx.doi.org/10.1016/j.rpor.2016.06.004
1507-1367/

1. Background

Surgical resection remains the main treatment for liver cancer, including hepatocellular carcinoma (HCC), bile duct cancer and liver-confined metastases. For inoperable tumors, several treatment options including chemo-embolization and ablative techniques as radiofrequency have been evaluated.[1–4]

The use of radiotherapy (RT) for unresectable liver cancer, has been limited because of the risk of radiation-induced liver disease (RILD) which may occur after low-dose whole liver irradiation.[5,6] However, nowadays it is well known that as the liver is organized in parallel functional subunits, toxicity is correlated to the irradiated volume, and the delivery of high doses of radiation to a restricted liver volume can be well tolerated if the remaining normal liver parenchyma is spared.[7–9]

Stereotactic body radiotherapy (SBRT) allows the delivery of a high dose of radiation to the target, using either a single dose or a small number of fractions with a high degree of precision within the body.[10] But despite this potential high accuracy offered by the technique, one of the major challenges in SBRT is the motion management of thoracic and abdominal tumors that translates in a potential target miss induced by breathing. Attempts to control or to compensate for liver motion are essential for stereotactic liver radiotherapy since dose escalation has been associated with improved local control and survival in prior radiation series.[11–13]

In an attempt to manage or compensate for motion, several studies of liver SBRT have been published using SBF (Stereotactic Body Frame) with abdominal compression or breath hold technique with spirometer, associated with in-room and/or on-board imaging for treatment verification (MV portal imaging, KV radiographic and fluoroscopy acquisition, KV and MV cone-beam computed tomography (CBCT), 4-dimensional (4D) CBCT, etc.), in most cases for a pre-treatment set-up.[14–18] But those approaches have some inconvenient, leading to possible target miss. First, due to the fact that they are associated with external information not directly correlated to the tumor motion; and second, because of the impossibility to asses changes in the amplitude of breathing motion that may occur during some fractions, using only pretreatment imaging verification. Furthermore, some of these techniques, as they need patient's collaboration, are not feasible or cannot be applied due to a bad clinical tolerance.[19] The most interesting technique is certainly intrafraction treatment verification, since small external geometric errors, which may be translated in large deviations in the delivered dose distribution, could be detected and then avoided.[20,21]

This continuous verification of the target position is a key point for all the delivery techniques and could be applied with gating, tracking or free breathing treatment.

There is actually no available commercial solution using on-line information about the target position acquired by imaging to adapt "in flight" the treatment delivery. The best approach proposed by different companies involved in radiation therapy is globally the same. It involves following a surrogate representing the tumor motion but not the target itself during treatment and checking this real tumor position using imaging with a frequency depending on the system used. All the systems actually build a model before the treatment, representing the correlation between the external information followed by the delivery system and the internal information. External information represents the breathing pattern and is acquired by different systems (jacket or box on the patient with reflective markers, elastic belt). Internal information represents target position visualized on image acquisition (4DCT, 4DCBCT, KV images). During the last decade, tracking had been implemented on a robotic system (Cyberknife Accuray Inc., Sunnyvale, CA) in which the system follows the information delivered by reflective balls attached to a jacket on the patient and verifying the accuracy of the target position by stereoscopic KV X-ray images between irradiation, meaning between two positions (node) of the system but not during the beam delivery.[22]

Recently some technological advances allowed real-time position verification simultaneously to beam delivery for targets undergoing respiratory motion during arc radiotherapy for conventional gantry mounted linear accelerators.[23]

This technique could be used for free breathing treatment and for gating delivery that limits the radiation beam to selected parts of the breathing cycle, allowing dose escalation to the tumor and dose reduction to surrounding tissues. Li et al.[24] reported intrafraction verification of respiration-gated RapidArc SBRT. They showed significant deviations of fiducial markers from the expected position by more than 2 mm, emphasizing the need for gating techniques with beam on-off synchronized on markers position instead of systems monitoring the position of the tumor with external surrogates.

Here we present our study of liver SBRT on a free breathing mode, using intrafraction motion review (IMR, Varian medical system) which allows simultaneous KV information and MV delivery to analyze motion management and synchronizes the beam during gated RapidArc allowing a reduction in the required PTV margin, facilitating dose escalation.

Preliminary clinical results are provided.

2. Materials and methods

2.1. *Patients characteristics*

Between May 2012 and March 2015, 41 consecutive patients were treated by SBRT using a gated RapidArc technique with a Varian Novalis Truebeam STX® linear accelerator v.1.6. Mean age was 69 years (range 47–85). Among them, 37 were treated with a radical intent and 34 patients with 42 lesions were analyzed for clinical results. 11 patients were treated for hepatocellular carcinoma, 5 for cholangiocarcinoma, 17 for liver metastases from colorectal cancer and 1 patient for liver metastases from breast cancer. Twelve patients had cirrhosis. Among them, eleven were child A and one child B. Most patients had been heavily pretreated and liver stereotactic body radiotherapy was proposed when no other local therapy, such as surgery, radiofrequency or chemo-embolization, was advisable. The median number of previous chemotherapy lines was 3 (range 1–4) for colorectal patients, and two for cholangiocarcinoma patients. Median number of previous liver surgeries for colorectal patients was 2 (range 1–4). Among them, two patients also received a radiofrequency treatment before radiotherapy. All patients with hepatocellular

Table 1 – Patients characteristics.

Characteristics	n	%
n° patients (follow-up ≥ 6 months)	34	
Mean age	69 (42–90)	
n° lesions	42	
Patients with liver metastasis	18	53
Sein	1	3
Colorectal	17	50
Primary hepatobiliary tumors	16	47
Cholangiocarcinoma	5	15
Hepatocellular carcinoma	11	32
Cirrosis at diagnosis (Child–Pugh class)	12	
CHILD A	11	
CHILD B	1	
Dose/fractionnation		
10 × 4 Gy (2 weeks)	1	
5 × 10 Gy (1 week)	16	
5 × 10 Gy (2 weeks)	3	
10 × 5 Gy (2 weeks)	14	
GTV location by hepatic segment		
I	4	9
II	1	2
III	0	0
IV	6	15
V	2	5
VI	1	2
VII	4	10
VIII	12	29
Hepatectomy scar	1	2
Multiple or overlapping segments	8	19
nd	3	7
GTV contact with vessels		
VCI	10	35
Portal	14	48
Hepatic	5	17

carcinoma were inoperable and 6 and 3 of them had a previous radiofrequency or chemoembolization, respectively. Most of the patients had only liver metastases or limited distant metastases to the lungs. Radiotherapy dose ranged from 40 to 50 Gy in 5–10 fractions. The prescribed dose and number of fractions were chosen depending on hepatic function, irradiated liver volume and dose-volume histograms results. Patient characteristics are shown in Table 1.

Toxicity was evaluated using CTC v.04 classification. Treatment response was evaluated by CT scan and RMN.

2.2. *SBRT technique*

2.2.1. *Patient simulation*

Patients were placed for treatment in supine position with their arms above their heads, using a special support and a personalized back pillow fitting the patient shape (moldcare Sinmed, The Netherlands). They underwent three to four 4-dimensional computed tomography (4DCT) scans acquired in a cine mode with a 16 slices General Electric (GE) RT Scanner to verify the reproducibility of the target motion. Axial slice thickness acquisition was 1.25 mm reconstructed in 2.5 mm. These CT scans were realized at least 7 days after implantation of 2–3 fiducial markers into the liver, in or nearby the tumor, to help patient set-up and online treatment verification. 4DCT scans were acquired using Real time Position Management system (RPM, Varian Medical Systems, Palo Alto, CA) recording the breathing signal. The first among the four acquisitions consisted in a rapid CT with iodine injection. This allowed the radiation oncologist to better define the GTV due to the contrast-enhancement of the target. The cine 4D CT images were separated into 10 phases CT series ($P_{0\%}$ to $P_{100\%}$) based on respiratory motion information, using the Advantage 4D applications (General Electric Medical system). A Maximum Intensity Projection (MIP) and an Average Intensity Projection (Ave-IP) CT series were generated to make it possible to generate the treatment planning and to collect fiducial motion information during the whole breathing cycle.

A magnetic resonance imaging (MRI) was acquired in treatment conditions with a flat table in the exhale and inhale phase and co-registered to the contrast-enhanced CT scan to improve the gross tumor volume definition (GTV). the second step was to evaluate all the CT phases ($P_{0\%}$ to $P_{100\%}$) to find the one where the fiducial position was comparable to the position in the injected CT. Starting from this reference position, we studied the maximal displacement of the fiducial on the 3 space directions. This gave us an adequate margin to apply to the GTV to define the Internal Target Volume (ITV). Then a continuous motion of the different CT phases was played to validate if the GTV motion was totally included in the ITV. The Planning Target Volume (PTV) was then created by adding a 5 mm margin to the ITV. Next, few steps were necessary to define specific positions of the fiducial markers for patient positioning and tumor motion verification in the treatment room. The global motion of the fiducial marker was outlined in the MIP CT series as well as the specific position of the markers in maximal exhalation ($P_{50\%}$) and inhalation phases ($P_{100\%}$) for online verification.

A virtual point structure was created in the treatment planning system software to be a reference for each fiducial marker. This point was placed at the center of the fiducial marker, lying exactly at the threshold of the planned treatment, for gating at the exhale and inhale phases.

The treatment planning was realized based on the Ave-IP CT series where the organs at risk (OAR) were contoured. Dose constraints were defined as shown in Table 2.

Treatment delivery was done by volumetric modulated arc-therapy (VMAT) on a Truebeam Novalis STX® provided with a high definition multileaf collimator. Leaf thickness was 2.5 mm for the first 20 leaves from the central axis and 5 mm for the others. Two arcs were generally used with a starting point at ±60° and finishing one at 180°. Collimator rotation was systematically 45° for the first arc and 315° for the second. No high dose rate using flattening filter free beams were used for this group of patients.

Before each treatment fraction delivery, the RPM block was placed on the patient's abdominal surface at the same position as in the planning CT, and the gating signal was generated by the RPM system. No reference RPM signal coming from a different 4D CT simulation was used. The gating window was then adjusted to encompass the breathing signal of the day and a CBCT was acquired. This CBCT imaging (acquisition time of 1 min) which provided an average information, was compared to the AVE IP CT used for the planning to ensure that the representation of the fiducial matched perfectly the contour drawn on the MIP image. The patient's alignment set was based first on external body, bones and soft tissue structures and then

Table 2 – Dose constraints.

OAR	5 fractions	>5 fractions
Liver–PTV	D_{max} < 15 Gy >700 cc if liver volume > 2000 cc $D_{35\%}$ < 15 Gy If liver volume < 2000 ml	
Liver–GTV	D_{max} < 15 Gy >700cc if liver volume > 2000cc D_{mean} < 13 (primary tumor) D_{mean} < 15 (metastasis)	D_{mean} < 18 Gy (primary T) D_{mean} < 20 Gy (metastasis)
Kidneys	V_{18Gy} < 33% D_{moy} as less as possible One kidney and creatinine > 2.0 mg/dl) ≥ $D_{10\%}$ < 10 Gy	
Spinal cord	D_{max} < 25 Gy $V_{22.5Gy}$ < 0.25 cc $V_{13.5Gy}$ < 1.2 cc	
Heart	D_{max} < 35 Gy/38 Gy V_{32Gy} < 15 cc	
Stomach	D_{max} < 31 Gy V_{28Gy} < 10 cc	
Duodenum	D_{max} < 31 Gy V_{18Gy} < 5 cc	
Small Bowel	D_{max} < 29 Gy $V_{19.5Gy}$ < 5 cc	
Bowel	D_{max} < 29 Gy V_{25Gy} < 5 cc	
Esophagus	D_{max} < 35 Gy $V_{19.5Gy}/_{27.5Gy}$ < 5 cc	
Ribs	D_{max} < 43 Gy V_{35Gy} < 1 cc	

on the fiducial markers. This CBCT was important to check the global amplitude of the ITV. In the second step we realized a kV/kV matching that gave us information about the extreme positions. The gating window was manually adjusted, defining a threshold to slightly cut the breathing signal in such a way that the KV beam on/off came about when the breathing signal cut one of the defined thresholds ($P_{50\%}$ and $P_{100\%}$). Once the image acquisition was done, we compared the expected position of the fiducial in these special phases defined during treatment planning to the real position of the marker in the acquired image. This adjustment using KV/KV on the specific positions limiting the gating window ensured that when the MV beam was enabled, the markers (target) were in the same position as in the planning. Furthermore, accuracy of the positioning was increased compared to the CBCT, due first to a fixed and not blurred image (no motion in the KV snapshot compared to CBCT) and second to the spatial resolution coming from 2.5 mm reconstructed slices to 0.585 mm/pixel with the imager at 150 cm from the source.

Using the same process during the treatment, intrafraction kV images were acquired at each exhalation and inhalation phase of the breathing cycle and the positions of the fiducial markers were compared with their expected positions, represented by the created virtual point (Fig. 1).

In the case of a lack of accuracy, because of changes in the patient's breathing cycle amplitude or a modification of the correlation between external surrogate and internal markers, the gating threshold could be modified until fiducial markers lied exactly in the expected position (see in this issue: *Evaluation of consistency of tumor repositioning during multiple breathing cycles for liver stereotactic treatment*).[25]

3. Results

Between May 2012 and March 2015, 41 patients were treated with liver stereotactic radiation therapy with VMAT-Rapidarc using an intrafraction motion review.

3.1. *Dosimetric results*

Dose constraints were respected in most cases except when PTV location was extremely close to OAR in which case the maximum planned doses were punctually exceeded. This was

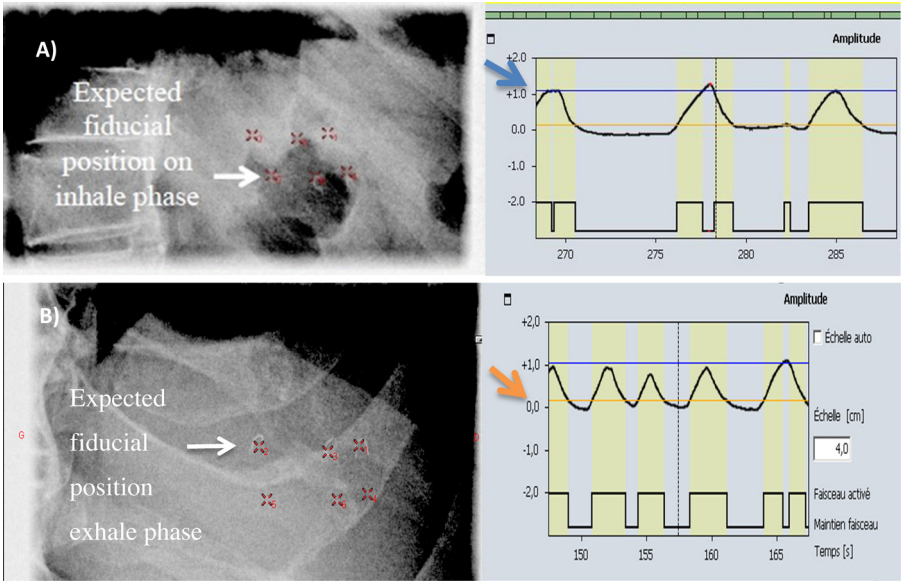

Fig. 1 – Fiducials position verification respective to the expected position in the inhale (A) and exhale (B) phase.

Table 3 – Dosimetric results.

	Mean	Max	Min
PTV			
V_{PTV} (cc)	182.56	820.60	24.60
$V_{Iso\ 95\%}$ (cc)	175	834	24
$D_{98\%}$ (Gy)	45.89	49.06	30.41
$D_{2\%}$ (Gy)	50	52.52	35.8
Liver			
$V_{Liver\ excludding\ PTV}$ (cc)	1510.72	3057.20	946
$V_{<15\,Gy>700\,cc}$ (cc)	925.42	2736.20	0.00
Kidney			
Rigth Kidney D_{mean} (Gy)	1.73	7.40	0.27
$V_{18\ Gy}$ (%)	1.86	28.68	0
Left Kidney D_{mean} (Gy)	0.71	3	0.03
$V_{18\,Gy}$ (%)	0	0	0
Spinal cord dose (Gy)	7	18	1.80
Digestive tract			
D_{max} (Gy)	18.75	46.30	0.60
D_{mean} (Gy)	2.20	6.03	0.13
$V_{25\ Gy}$ (cc)	1.05	17.37	0.00
Duodenum			
$D_{25\ Gy}$ (cc)	1.15	19	0
D_{max} (Gy)	13.95	47.91	0.60
D_{mean} (Gy)	2.86	10.47	0.33
Stomach			
D_{max} (Gy)	15.96	45.10	2.20
D_{mean} (Gy)	4.35	10.26	0.29
V_{27Gy} (cc)	0.75	19.60	0.00
Esophagus			
D_{max} (Gy)	16.65	39.80	0.45
D_{mean} (Gy)	7.48	22.54	0.16
Heart			
D_{max} (Gy)	15.74	48.20	0.17
D_{mean} (Gy)	2.31	6.83	0.07

the case of patients with liver tumors touching the stomach, duodenum, esophagus and heart. In those situations fractionation was adapted. Numerical analysis of dosimetric results is shown in Table 3.

3.2. *Technical results*

50 fractions corresponding to 5 fractions per patient above the first 10 patients were evaluated, and results are shown in Table 4. Mean number of KV images per arc was 35 (range 7–74). Mean fraction time delivery (room use) was 53 min for the first fraction, but it was reduced until 24 min after the second or third fraction.

For the 10 PTV patients, the average (±SD) conformity index defined as $(V_{PTV\ 95\%}/V_{PTV})^{*}(V_{PTV\ 95\%}/V_{95\%})$ was 0.93 ± 0.02, and homogeneity index defined as $(D_{2\%} - D_{98\%})/D_{mean}$ was 0.08 ± 0.02.

Mean intrafraction deviation of fiducials with respect to the expected position in the craneo-caudal direction was 0.91 mm (range 0–6 mm).

The estimated additional dose delivery due to the imaging verification was for CBCT 17.7 mGy (CTDIw) and 0.3 mGy for KV for tube parameters of 80 kV and 4 mAs.

A more exhaustive analysis of 2705 images corresponding to the first five fractions of treatment in our first ten patients is published in this issue for additional information concerning tumor repositioning (see in this issue: *Evaluation of consistency of tumor repositioning during multiple breathing cycles for liver stereotactic treatment*. Bedos L. et al.).[25]

3.3. *Clinical results*

Clinical results were evaluated for 34 patients. Median follow-up was 13 months (4–32 months). A total of 42 lesions were treated with a mean size of 33.4 mm (range 12–90 mm). The mean PTV volume was 175.90 cc (24–820 cc). Mean liver volume excluding PTV was 1479.33 cc (792.10–3057.20 cc). The treatment was well tolerated and no patient presented RILD, perforation or gastrointestinal bleeding. As regards acute toxicity: 11.7% (4/34) of patients presented G1 abdominal pain, 5.8% (2/34) had nausea, 29.4% (10/34) had G1 and 3% (1/34) G2 asthenia. 31% (6/19) of evaluable patients for liver function presented an asymptomatic perturbation of liver enzymes within 3 months after radiotherapy that was transitory in most of the cases. 1 patient had liver decompensation (the only patient who had antecedent of CHILD-B).

In-field control at 6 months was evaluable in 31 patients and was 90.32%. There were 7 complete responses (22.58%), 14 partial responses (45.17%), 7 stabilizations (22.58%) and 3 in field progressions (9.67%). Three patients out of the 7 who stabilized and other 2 patients out of the 14 with partial responses had progression after 9–12 months and 18–27 months, respectively. A total of 8 patients presented "in field" progression following radiotherapy. Twelve patients had an intrahepatic progression "out of field". Thirteen patients evolved with extrahepatic metastatic disease. No correlation could be established between relapse and PTV volume or dose in this study.

4. Discussion

Our results showed a high accuracy in dose delivery using gated RapidArc and intrafraction KV images, with a mean intrafraction deviation of fiducials with respect to the expected position in the craneo-caudal direction of 0.91 mm showing a satisfactory motion control during beam delivery.

Intrafraction control is essential to guarantee high accuracy beam delivery with preservation of surrounding healthy

Table 4

Fraction number	1	2	3	4	5
Time/fraction (min)	53	30	20	24	24
Mean number of KV images/arc	34 [9–56]	32 [7–60]	36 [12–56]	40 [28–74]	34 [18–48]
Mean deviation in the cranio-caudal sence (mm)	1.00 [0–5]	0.79 [0–5]	0.81 [0–4]	1.06 [0–6]	0.91 [0–5]

tissues. Most of the available techniques offer imaging control of the tumor position before and/or after, but not during the beam delivery.

The problem is that in spite of regular breathing, it some liver displacements may be observed, especially in the superior–inferior (SI) direction, in the range of 5–50 mm that could imply, in the absence of an intrafraction control, a target miss if adequate margins are not planned.[26,27] Although several techniques, like the use of active breath control devices (allowing a gated beam delivery) and Stereotactic body frame (with or without an abdominal compression plate), have attempted to negate liver motion or to reduce it.[28–30]

The management of intrafraction variability in liver position remains aleatory.

Even if the use of abdominal compression has shown to reduce intrafraction variability in liver position,[19,31] it has been recognized that the patient and tumor position were subject to a day to day variation based on the observation of a poor correspondence between the bony and soft-tissue landmarks.[32–36] This was confirmed by Guckenberger M. et al. who conducted a 4D-IGRT study in liver SBRT with acquisition of a CBCT study immediately before and after treatment delivery. Despite successful immobilization of the patient with a SBF, they observed considerable drifts in the target position independently from the bony anatomy in an order of 3.7 ± 2.2 mm on average. Furthermore, they confirmed that the position relative to the bony anatomy did not remain constant with changes in the motion amplitude of >3 mm seen in 17% of the treatment fractions and it could be >5 mm in patients treated without abdominal compression.[31] Those findings denoted, as previously reported by Wulf et al., the need of security margins to compensate these intrafractional uncertainties of at least 6 mm in the SI direction and 4 mm in the Left-Right (LR) direction.[35]

Another approach is the use of respiratory gating, which is considered accurate only when internal tumor motion occurring during beam-on, does not exceed treatment margins.[37] The problem is that, as we mentioned before, the breathing cycle is not strictly regular, but varies in amplitude and period from one cycle to another.[38–40] In addition, there will be some residual tumor motion which may exceed the allowed motion range. Large fluctuations (>300%) have been observed in the residual motion between some beams and, although gating may reduce the total tumor motion, the residual motion behaves unpredictably. Following these observations, some investigators concluded that it was mandatory to use individualized treatment margins that account for motion and realization of daily imaging to ensure that the residual motion does not exceed the planned motion on a given day.[41–43] Even for patients treated with abdominal compression, during the treatment, the residual tumor motion could be closer to 7–8 mm peak to peak, and it was observed that a shift in the baseline of the motion could increase the total residual motion of the tumor.[44] This was confirmed by Worm et al. who observed that "Intrafraction displacements increased slightly as a function of time and large intrafield breathing motion indicated an increased risk of large baseline shifts without impact in the use of abdominal compression to guarantee subcentimeter intrafield motion or baseline shifts.[45]

Ge et al.[46] evaluated possible uncertainties in the accuracy of respiratory gating comparing pair fluoroscopic movies acquired from 12 abdominal patients pre- and post-treatment. The change of global EIC (external–internal correlation) over time was identified as the largest contributor for gating uncertainty (in 43% of the cases). The second largest factor for gating uncertainty was suboptimal gating setup (found in 37% of the cases). As they studied only pre and post-treatment data, they recognized missing data during treatment delivery, and concluded that a continuous verification of EIC during treatment combined with computer-optimized gating parameters holds potential to further reduce PTV margin and improve gating accuracy. This comfort us in the choice of our technique that has the advantage of providing real tumor position information during beam delivery and makes sure that the tumor stays well covered by the radiation beam during the treatment delivery, allowing reduction of PTV margins and the possibility of dose escalation.

To date, tumor tracking has been implemented clinically only for the robotic Cyberknife system (Accuray Inc., Sunnyvale, CA) in which the required intratreatment target position signal is obtained by stereoscopic KV X-ray images of implemented markers. Image acquisition, target localization, and alignment corrections are repeated continually during treatment delivery, typically every 30–60 s.[22] But most patients will have breathing cycles of 3–4 s during which the tumor can move 1–3 cm. Most of the motion occurs in less than 1 s. Thus, the detection and response to motion must occur in much less than 1 s. This requires fast position measurement and algorithms that can accurately predict the breathing cycle up to several hundred milliseconds in advance.[47] If the target position is deduced from a surrogate breathing signal, the uncertainty in predicting the future tumor position is compounded by the uncertainty in relating target and surrogate motion.

Poulsen et al. demonstrated the feasibility of DMLC target tracking based on a single imager for RapidArc radiotherapy of tumors undergoing respiratory motion with accuracy below 2 mm for most trajectories.[23] More recently, Li et al.[24] evaluated the accuracy of gated RapidArc treatment using intrafraction KV images. They showed that the average 3D distance between the markers and their expected position (that they named ITVs) was 0.8 ± 0.5 mm (range 0–1.7 mm). They estimated that a left-right margin of 0.6 mm, an anterior–posterior margin of 0.8 mm, and a superior–inferior margin of 1.5 mm was required to account for 95% of the intrafraction uncertainty in RPM-based RapidArc gating. For some patients, the markers were outside the ITV by more than 2 mm at the beginning of the MV beam-on which emphasizes the need for gating techniques with beam on-off controlled directly by an actual position of the tumor target instead of external surrogates such as RPM.[48,49] They studied the possible explications for error repositioning including the Truebeam mechanical and imaging accuracy and they concluded that patient's breathing was the main factor affecting the gating error.

Those results are concordant with our study. We used a similar technique allowing two Kv images in every breathing cycle that gave us true information about what was really happening during treatment delivery and comfort the chosen PTV margin. Furthermore, this technique allowed us to adapt, in real time if necessary, the gating window threshold and patient setup.

In our study we observed that in some fractions the fiducials deviation respective to the expected position reached up to 5 mm, showing that even within the same treatment phase, there exists an intrafraction motion or a miss of reproducibility of the target motion from one breathing cycle to the other. This confirms the importance of controlling breathing related motion in liver SBRT to guarantee adequate target coverage and spare the nearby organs at risk. Since the margin we used to extend the ITV to the PTV was of 5 mm, the target remained always covered during the whole beam delivery. And even if a greater deviation was observed, as this could be detected during the beam delivery, we were able to adapt the treatment gate and the patient's set-up.

One limitation of our study is the evaluation of fiducial motion only in the Supero–Inferior (SI) direction. But we made this choice because most of the authors evaluating 3D-Intrafraction and Interfraction motion have described that the largest intrafraction motion occurs in this direction.[31,43,45,50–52] Ge et al. reported that although the respiratory-induced tumor motion was found to be the largest in the SI direction, the impact of AP motion on gating accuracy could be non-negligible if the patient was not set up optimally in that direction.[46]

In our study, mean fraction delivery time (room occupation) was 53 min for the first fraction, but time was dramatically reduced down to 24 min after the second or third fraction. This was not longer than delivery time found in the literature, that is around 45 min, even without real-time intrafraction verification.[31,45,50]

Regarding clinical results, we obtained 6 months "in field" control of 90.3% and a rate of 21.7% of complete responses with a very low toxicity profile. Meyer et al.,[53] in a phase I study of dose escalation for liver metastases from different primary sites, obtained a rate of 2.5 year local control (LC) of 100% using 1 fraction of 35 Gy for seven patients and escalated to 40 Gy for seven additional patients. Tumors were located outside of the central region. Median PTV volume was 27.95 ml (range 4.08–79.34 ml). They did not observe ≥G3 toxicity. Mendez-Romero et al. are publishing in this special issue[54] their experience in treating liver metastases using two fractionation schedules (37.5 and 50.25 Gy in 3 fractions prescribed to the 65–67% isodose). Tumor size was <6 cm. Local control was better for the highest doses group even if this difference did not reach significance. 1 – One-year LC was 96% vs. 90%; 2 – year LC was 74 vs. 90% and tree-year LC was 66 vs. 81%. Toxicity was limited and not increased in the highest dose group. Scorsetti et al.[55] published a phase II study for liver metastases using 3 fractions of 25 Gy with a two-year local control of 91%. Median tumors size was 3.5 cm (range 1.1–5.4 cm). No grade ≥3 toxicity was observed.

Other series have evaluated local control when treating hepatocellular carcinoma. Bujold et al.,[56] in a phase I-II study of dose escalation using 24–54 Gy in 6 fractions, obtained a LC of 87% at 1 year. There were 11% CR, 43% of PR and 44% of stabilization. In univariate analysis minimum dose to the PTV was a significant factor for local control. No grade ≥3 toxicity was observed. Jang et al.[57] evaluated two SBRT doses 33 Gy in 3 fractions and 60 Gy in 3 fractions for treating HCC. Tumors were ≤7 cm. 2-year LC was 87%. For tumors <5 cm, LC was 90% and for >5 cm, it was 63% ($p = 0.015$); when dose was higher than 54 Gy, LC was 100%, for doses between 45 and 54 Gy, LC was 78% and for doses below 45 Gy 64%. LC at 5 years was 82%.

Our study showed encouraging results with an "in field" control of 90.3% at 6 months but needs a longer follow up to evaluate LC results at 1 and 2 years. Based on the literature above, the most important factor for local control was the delivered dose to the PTV and the size of treated tumors even if those factors did not reach statistical significance in all the studies. In our series, patients were very heavily pretreated; tumors were big and in many cases the liver volume excluding PTV was restricted. That is why, we started to deliver a moderate hypofractionation and total dose. Despite these unfavorable situations, we could furnish a satisfactory and well tolerated treatment for those patients. In the future, and being secured by the accuracy of our technique, our objective will be to increase the dose per fraction and the total dose in an attempt to improve long term local control.

5. Conclusion

Imaged-Guided liver SBRT using VMAT and real-time adaptive tumor gating is feasible and offers a high accuracy in dose delivery. A PTV margin of 5 mm around the ITV was largely enough to cover the target volume. Further analysis will allow us to diminish the PTV margin around the ITV. Delivery treatment time was not prolonged by the fact of obtaining intrafraction Kv images when compared to other liver SBRT techniques.

The clinical tolerance was satisfactory without presentation of RILD despite the high volumes treated. In-field control was satisfactory but dose escalation will be evaluated in the continuity of this study.

Conflict of interest

None declared.

Financial disclosure

None declared.

REFERENCES

1. Bruix J, Sherman M. American Association for the Study of Liver Diseases. Management of hepatocellular carcinoma: an update. *Hepatology* 2011;**53**(3):1020–2.
2. EASL-EORTC clinical practice guidelines: management of hepatocellular carcinoma. *Eur J Cancer* 2012;**48**:599–641.
3. Koo T, Kim J. Extrahepatic bile duct cancer: analysis of treatment outcomes and patterns of failure. *Int J Radiat Oncol Biol Phys* 2012;**84**(3):S325–6.
4. Salinski S, Zalinski a S, Marietteb C, et al. Management of patients with synchronous liver metastases of colorectal cancer. Clinical Practice Guidelines. Guidelines of the French society of gastro-intestinal surgery (SFCD) and the association of hepatobiliary surgery and liver transplantation (ACHBT). Short version. *J Visc Surg* 2011;**148**, xxx.e171–xxx.e182.

5. Lawrence TS, Lawrence TS, Robertson JM, et al. Hepatic toxicity resulting from cancer treatment. *Int J Radiat Oncol Biol Phys* 1995;**31**(5):1237–48.
6. Russell AH, Clyde C, Wasserman TH, Turner SS, Rotman M. Accelerated hyperfractionated hepatic irradiation in the management of patients with liver metastases: results of the RTOG dose escalating protocol. *Int J Radiat Oncol Biol Phys* 1993;**27**:117–23.
7. Hall EJ. *Radiology for the radiologist*. 5° ed. dir Lippincott, Williams &Wilkins; 2000. p. 314–36.
8. Guha C, Sharma A, Gupta S, et al. Amelioration of radiation-induced liver damage in partially hepatectomized rats by hepatocyte transplantation. *Cancer Res* 1999;**59**(December (23)):5871–4.
9. Emami B, Lyman J, Brown A, et al. Tolerance of normal tissue to therapeutic irradiation. *Int J Radiat Oncol Biol Phys* 1991;**21**(May (1)):109–22.
10. American Society for Therapeutic Radiology and Oncology, American College of Radiology. Potters L. Practice guideline for the performance of stereotactic body radiation therapy. *Int J Radiat Oncol Biol Phys* 2004;**60**:1026–32.
11. Ben-Josef E, Normolle D, Ensminger WD, et al. A Phase II trial of high dose conformal radiation therapy with concurrent hepatic artery fluorodeox-yuridine for unresectable intrahepatic malignancies. *J Clin Oncol* 2005;**23**(December (34)):8739–47.
12. Seong J, Park HC, Han KH, Chon CY. Clinical results and prognosis factors in radiotherapy for unresectable hepatocellular carcinoma: a retrospective study of 158 patients. *Int J Radiat Oncol Biol Phys* 2003;**55**(February (2)):329–36.
13. Jang WI, Kim MS, Bae SH, et al. High-dose stereotactic body radiotherapy correlates increased local control and overall survival in patients with inoperable hepatocellular carcinoma. *Radiat Oncol* 2013;**8**(October):250.
14. Wang Z, Nelson JW, Yoo S, et al. Refinement of treatment set-up and target localization accuracy using three-dimensional cone-beam computed tomography for stereotactic body radiotherapy. *Int J Radiat Oncol Biol Phys* 2009;**73**(2):571–7.
15. Pouliot J, Bani-Hashemi A, Chen J, et al. Low-dose megavoltage cone-beam CT for radiation therapy. *Int J Radiat Oncol Biol Phys* 2005;**61**(February (2)):552–60.
16. Sonke JJ, Zijp L, Remeijer P, van Herk M. Respiratory correlated cone-bean CT. *Med Phys* 2005;**32**(4):1176–86.
17. Li T, Xing L, Munro P, et al. Four-dimensional cone-beam computed tomography using an on-board imager. *Med Phys* 2006;**33**(10):3825–33.
18. Jayachandran P, Minn AY, Van Dam J, Norton JA, Koong AC, Chang DT. Interfractional uncertainty in the treatment of pancreatic cancer with radiation. *Int J Radiat Oncol Biol Phys* 2010;**76**(February (2)):603–7.
19. Case RB, Sonke JJ, Moseley DJ, Kim J, Brock KK, Dawson LA. Inter and intrafraction variability in liver position in non-breathing hold stereotactic body radiotherapy. *Int J Radiat Oncol Biol Phys* 2009;**75**(September (1)):302–8.
20. Dawson LA, Eccles C, Bissonnette JP, Brock KK. Accuracy of daily image guidance for hypofractionated liver radiotherapy with active breathing control. *Int J Radiat Oncol Biol Phys* 2005;**62**(July (4)):1247–52.
21. Méndez Romero A, Zinkstok RT, Wunderink W, et al. Stereotactic body radiation therapy for liver tumors: impact of daily setup corrections and day-to-day anatomic variations on dose in target and organs at risk. *Int J Radiat Oncol Biol Phys* 2009;**75**(November (4)):1201–8.
22. Kilby W, Dooley JR, Kuduvalli G, Sayeh S, Maurer Jr CR. The Cyberknife robotic radiosurgery system in 2010. *Technol Cancer Res Treat* 2010;**9**(October (5)):433–52.
23. Poulsen PR, Cho B, Ruan D, Sawant A, Keall PJ. Dynamic multileaf collimator tracking of respiratory target motion based on a single kilovoltage imager during arc radiotherapy. *Int J Radiat Oncol Biol Phys* 2010;**77**(June (2)):600–7.
24. Li R, Mok E, Chang DT, et al. Intrafraction verification of gated RapidArc by using beam-level kilovoltage X-ray images. *Int J Radiat Oncol Biol Phys* 2012;**83**(5):e709–15.
25. Bedos L, Olivier R, Norbert A, et al. Evaluation of reproducibility of tumor repositioning during multiple breathing cycles for liver stereotactic body radiotherapy treatment. *Rep Pract Oncol Radiother* 2017;**22**(2):132–40.
26. Balter JM, Dawson LA, Kazanjian S, et al. Determination of ventilator liver movement via radiographic evaluation of diaphragm position. *Int J Radiat Oncol Biol Phys* 2001;**51**(September (1)):267–70.
27. Davis SC, Hill AL, Holmes RB, Halliwell M, Jackson PC. Ultrasound quantitation of respiratory organ motion in the upper abdomen. *Br J Radiol* 1994;**67**:1096–102.
28. Hawkins MA, Brock KK, Eccles C, Moseley D, Jaffray D, Dawson LA. Assessment of residual error in liver position using KV cone-beam computed tomography for liver cancer high-precision radiation therapy. *Int J Radiat Oncol Biol Phys* 2006;**66**(October (2)):610–9.
29. Dawson LA, Brock KK, Kazanjian S, et al. The reproducibility of organ position using active breathing control (ABC) during liver radiotherapy. *Int J Radiat Oncol Biol Phys* 2001;**51**(December (5)):1410–21.
30. Wunderink W, Wunderink W, Méndez Romero A, et al. Reduction of respiratory liver tumor motion by abdominal compression in stereotactic body frame, analyzed by tracking fiducial markers implanted in liver. *Int J Radiat Oncol Biol Phys* 2008;**71**(July (3)):907–15.
31. Guckenberger M, Sweeney RA, Wilbert J, et al. Image-guided radiotherapy for liver cancer using respiratory correlated computed tomography and cone-beam computed tomography. *Int J Radiat Oncol Biol Phys* 2008;**71**(May (1)):297–304.
32. Lax I, Blomgren H, Näslund I, Svanström R. Stereotactic radiotherapy of malignancies in the abdomen: methodological aspects. *Acta Oncol* 1994;**33**(6):677–83.
33. Blomgren H, Blomgren H, Lax I, Näslund I, Svanström R. Stereotactic high dose fraction radiation therapy of extracranial tumors using an accelerator: clinical experience of the first thirty-one patients. *Acta Oncol* 1995;**34**(6):861–70.
34. Herfarth KK, Herfarth KK, Debus J, et al. Extracranial stereotactic radiation therapy: setup accuracy of patients treated for liver metastases. *Int J Radiat Oncol Biol Phys* 2000;**46**(January (2)):329–35.
35. Wulf J, Hädinger U, Oppitz U, Olshausen B, Flentje M. Stereotactic radiotherapy of extracranial targets: CT-simulation and accuracy of treatment in the stereotactic body frame. *Radiother Oncol* 2000;**57**(November (2)):225–36.
36. Lohr F, Debus J, Frank C, et al. Noninvasive patient fixation for extracranial stereotactic radiotherapy. *Int J Radiat Oncol Biol Phys* 1999;**45**(September (2)):521–7.
37. Keall PJ, Mageras GS, Balter JM, et al. The management of respiratory motion in radiation oncology report of AAPM Task Group 76. *Med Phys* 2006;**33**(October (10)):3874–900.
38. Liang P. Non-stationary of breath-by-breath ventilation and approaches to modeling the phenomenon. In: Semple SJG, Adams L, Whipp BJ, editors. *Modeling and control of ventilation*. New York, NY: Plenum; 1995. p. 117–21.
39. Benchetrit G. Breathing pattern in humans: diversity and individuality. *Respir Physiol* 2000;**122**(September (2–3)):123–9.
40. Hugelin A, Vibert JF. Is the respiratory rythm multistable in man respiratory control. In: Swanson GD, Grodins FS, Hughson RI, editors. *A modeling perspective*. New York, NY: Plenum; 1989. p. 353–9.

41. Berbeco RI, Nishioka S, Shirato H, Chen GT, Jiang SB. Residual motion of lung tumours in gated radiotherapy with external respiratory surrogates. *Phys Med Biol* 2005;**50**(August (16)):3655–67.
42. Fuji H, Asada Y, Numano M, et al. Residual motion and duty time in respiratory gating radiotherapy using individualized or population based windows. *Int J Radiat Oncol Biol Phys* 2009;**75**(October (2)):564–70.
43. Ionascu D, Jiang SB, Nishioka S, Shirato H, Berbeco RI. Internal–external correlation investigations of respiratory induced motion of lung tumors. *Med Phys* 2007;**34**(October (10)):3893–903.
44. Berbeco RI, Hacker F, Ionascu D, Mamon HJ. Clinical feasibility of using an EPID in CINE mode for image-guided verification of stereotactic body radiotherapy. *Int J Radiat Oncol Biol Phys* 2007;**69**(September (1)):258–66.
45. Worm Es, Høyer M, Fledelius W, Poulsen PR. Three-dimensional, time-resolved, intrafraction motion monitoring throughout stereotactic liver radiation therapy on a conventional linear accelerator. *Int J Radiat Oncol Biol Phys* 2013;**86**(1):190–7.
46. Ge J, Santanam L, Yang D, Parikh PJ. Accuracy and consistency of respiratory Gating in abdominal cancer patients. *Int J Radiat Oncol Biol Phys* 2013;**85**(March (3)):854–61.
47. Murphy MJ. Tracking moving organs in real time. *Semin Radiat Oncol* 2004;**14**(January (1)):91–100.
48. Wiersma RD, Wiersma RD, Mao W, Xing L. Combined KV and MV imaging for real-time tracking of implanted fiducial markers. *Med Phys* 2008;**35**(April (4)):1191–8.
49. Li R, Lewis JH, Cerviño LI, Jiang SB. A feasibility study of markerless fluoroscopic gating for lung cancer radiotherapy using 4DCT templates. *Phys Med Biol* 2009;**54**(October (20)):N489–500.
50. Wunderink W, Méndez Romero A, Vásquez Osorio EM, et al. Target coverage in image-guided stereotactic body radiotherapy of liver tumors. *Int J Radiat Oncol Biol Phys* 2007;**68**(May (1)):282–90.
51. Eccles CL, Patel R, Simeonov AK, Lockwood G, Haider M, Dawson LA. Comparison of liver tumor motion with and without abdominal compression using cine-magnetic resonance imaging. *Int J Radiat Oncol Biol Phys* 2011;**79**(February (2)):602–8.
52. Kirilova A, Lockwood G, Choi P, et al. Three-dimensional motion of liver tumors using cine-magnetic resonance imaging. *Int J Radiat Oncol Biol Phys* 2008;**71**(July (4)):1189–95.
53. Meyer JJ, Foster RD, Lev-Cohain N, et al. A phase I dose-escalation trial of single-fraction stereotactic radiation therapy for liver metastases. *Ann Surg Oncol* 2016;**23**(1):218–24.
54. Mendez-Romero A. Institutional experience in the treatment of hepatic metastases with SBRT. *Rep Pract Oncol Radiother* 2017;**22**(2):126–31.
55. Scorsetti M, Comito T, Tozzi A, et al. Final results of a phase II trial for stereotactic body radiation therapy for patients with inoperable liver metastases from colorectal cancer. *J Cancer Res Clin Oncol* 2015;**141**(3):543–53.
56. Bujold A, Massey CA, Kim JJ, et al. Sequential phase I and II trials of stereotactic body radiotherapy for locally advanced hepatocellular carcinoma. *J Clin Oncol* 2013;**31**:1631–9.
57. Jang WI, Kim M-S, Bae SH, et al. High-dose stereotactic body radiotherapy correlates increased local control and overall survival in patients with inoperable hepatocellular carcinoma. *Radiat Oncol* 2013;**8**:250.